

Resilience assessment of tunnels: Framework and application for tunnels in alluvial deposits exposed to seismic hazard

Zhongkai Huang^a, Dongmei Zhang^{a,**}, Kyriazis Pitilakis^b, Grigorios Tsinidis^c,
Hongwei Huang^a, Dongming Zhang^a, Sotirios Argyroudis^{d,*}

^a Key Laboratory of Geotechnical and Underground Engineering of Ministry of Education, Department of Geotechnical Engineering, Tongji University, Shanghai, 200092, China

^b Department of Civil Engineering, Aristotle University of Thessaloniki, Thessaloniki, Greece

^c Department of Civil Engineering, University of Thessaly, Volos, Greece

^d Department of Civil and Environmental Engineering, Brunel University London, London, United Kingdom

ARTICLE INFO

Keywords:

Tunnels
Resilience
Earthquakes
Fragility
Restoration
Functionality

ABSTRACT

Transport infrastructure is the backbone of the economy and society, while at the same time is exposed to multiple hazards. Previous natural disasters, including earthquakes, had a significant impact on transport networks with severe consequences for the users and supply chain. In this context, the resilience assessment of critical assets such as tunnels is of paramount importance for increasing safety and maintaining their functionality in seismic-prone areas. This study presents a practical resilience assessment framework for tunnels subjected to earthquakes. The proposed framework combines fragility and restoration functions, for assessing the robustness of tunnels exposed to different seismic scenarios, and the rapidity of the recovery considering different damage levels. The framework is applied to circular tunnels in alluvial deposits. A life-cycle resilience index is estimated, and the effects of soil conditions, tunnel burial depths, construction quality, and aging of the tunnel lining, on the resilience quantifications are examined and assessed. This effort contributes to the resilience-based design and management of tunnels and underground transport networks, and hence, facilitates decision-making and efficient allocation of resources by consultants, operators, and stakeholders.

1. Introduction

Seismic hazard constitutes an essential threat to tunnels in seismic-prone areas. Post-event reconnaissance studies [1–3] have proven that the exposure of tunnels to earthquakes may lead to significant direct and indirect economic and social losses. For instance, the 1995 Kobe earthquake in Japan caused major damage to tunnels, including the entire collapse of the Daikai station [1]. The 1999 Chi-Chi earthquake in Taiwan resulted in damage of 49 of the 57 mountain tunnels within 60 km of the epicenter, including minor to moderate level cracking and spalling in the tunnel lining, as well as severe damage of tunnel portals [4]. More recently, the 2008 Wenchuan earthquake in China caused severe lining spalling and, in some cases, the collapse of tunnels [3]. Examples from Europe, include the Bolu tunnel in Turkey in 1999, and the San Benedetto tunnel in Italy due to the Norcia earthquake in 2016 [5]. In both cases, significant transverse ring cracks were formed in the

concrete liner. It is found that the tunnel lining, tunnel portal, and pavement damage, are the most vulnerable parts of tunnels subjected to strong ground motion. Common types of damage include the collapse of the portal, lining collapse, lining spalling, pavement uplift, failure of sidewalls, water leakage, and cracks [6]. In this context, it is of paramount importance to assess and quantify the risk, as well as the resilience of tunnels exposed to seismic hazards, to increase their reliability, protect the societies and safeguard the economy.

Resilience is described as the ability to withstand, respond and rapidly recover from natural or manmade hazards [7], while the most common properties of infrastructure resilience include robustness, rapidity, redundancy, and resourcefulness [8]. In this respect, resilience is related to organizational, technical, social, and economic aspects [9]. The concept of resilience-based assessment of structures and critical infrastructure has been on the frontline of research in recent decades [10,11], while it is gradually introduced in the design practices and

* Corresponding author.

** Corresponding author.

E-mail addresses: dmzhang@tongji.edu.cn (D. Zhang), Sotirios.Argyroudis@brunel.ac.uk (S. Argyroudis).

<https://doi.org/10.1016/j.soildyn.2022.107456>

Received 18 March 2022; Received in revised form 3 July 2022; Accepted 21 July 2022

Available online 9 August 2022

0267-7261/© 2022 The Author(s). Published by Elsevier Ltd. This is an open access article under the CC BY license (<http://creativecommons.org/licenses/by/4.0/>).

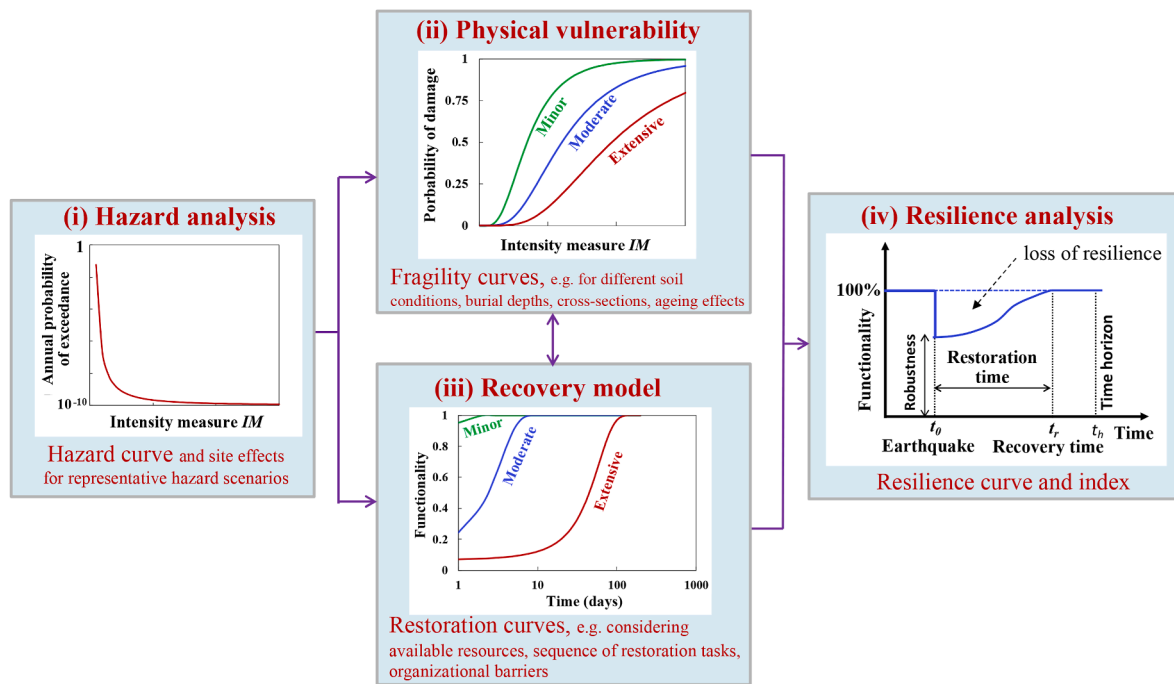


Fig. 1. Seismic resilience assessment framework of tunnels.

operational procedures of transport infrastructure stakeholders [12].

The quantification of infrastructure resilience is commonly associated with metrics or indexes, which measure the ability of the assets or networks to absorb damage, to recover after a failure, and to adapt to new conditions [11,13]. Metrics related to the resilience curve, which describes the robustness of a structure and the rapidity of its functionality recovery after an event, are widely used [14], while lifetime resilience considerations have been introduced into the life-cycle asset management [15]. Resilience assessment frameworks for single and multiple hazards have been proposed and applied, among others, for buildings [16,17], bridges [11,18,19], transport networks [20,21], and other critical infrastructure [22]. Resilience considerations for tunnels have been recently introduced by Huang and Zhang [23] in case of extreme surcharge, which is caused by the excessive dumped soils with a height of 5–8 m loaded on the ground surface without permission. However, to the authors' best knowledge, a framework for the quantification of the resilience of tunnels exposed to earthquakes has not been presented in the literature.

To bridge this knowledge gap, this study presents a practical resilience assessment framework for tunnels, which is then applied to circular tunnels in alluvial deposits exposed to ground seismic shaking. Furthermore, this study examines the effect of critical parameters on the vulnerability, and hence the resilience, of tunnels, such as the soil conditions, tunnel burial depths, construction quality of tunnels, and aging phenomena of the lining. Limitations of the proposed resilience assessment framework are discussed, whereas recommendations for further research are also discussed.

2. Seismic resilience framework for tunnels

Fig. 1 presents the proposed framework, which encompasses the steps of: (i) hazard analysis and definition of the hazard intensity, based on available hazard curves or other relevant studies for the examined tunnel sites, (ii) the physical vulnerability assessment, by adopting proper fragility functions (e.g., fragility curves), which assess the robustness of the structure and hence the loss of its functionality for given hazard intensities, (iii) the estimation of restoration time, which describes the rapidity of recovery after the occurrence of a hazard event,

by including adequate restoration models and (iv) the resilience analysis and quantification with resilience metrics. These steps are described in detail in the following sections.

2.1. Hazard analysis – hazard curve

Hazard can be characterized at the site of interest using a hazard intensity measure (IM) based on available hazard maps or curves or site-specific seismic microzonation studies [14]. In this way, the probability of exceeding a specified level of seismic demand in a given exposure period can be defined and/or the spatial distribution of the IM in case of site-specific response analysis for transport networks can be obtained. For tunnels, the surface peak ground acceleration (PGA) or the peak ground velocity (PGV), which is generally better correlated to structural damage, can be used to describe the seismic hazard intensity [24,25]. It is worth noting that the seismic performance and, hence, the damage states of tunnels are dominated by the imposed ground deformations during shaking. Meanwhile, PGV is closely related with the ground shear deformations (g_{max}) induced during ground shaking, as mentioned in NCHRP 611 report [26]. In this regard, PGV is better correlated with structural damage, and can be used as the intensity measure for assessing the fragility of the tunnel lining. This analysis step aims at defining representative seismic hazard scenarios for the tunnel site, for assessing the expected losses and the resilience of the infrastructure (steps ii and iv).

2.2. Physical vulnerability assessment - fragility functions

The seismic vulnerability of tunnels can be assessed based on fragility functions (e.g., fragility curves), which describe the conditional probability of being or exceeding a specific damage state for a given seismic intensity measure (IM) [27–29]. Empirical or analytical fragility functions may be used for the seismic vulnerability assessment of tunnels. Analytical approaches are more popular in resilience assessment since they are developed by employing numerical models, which can consider variable parameters and uncertainties related to the seismic demand and the capacity of the examined structure. Numerical models simulate the seismic response of the tunnel lining for a range of

Table 1
Potential patterns of damage on tunnels for various damage states [27,31,32].

Tunnel damage state (ds_i)	Damage patterns		Crack specification	
	Tunnel lining	Tunnel portal	Length (m)	Width (mm)
ds_0 , no damage	-	-	-	-
ds_1 , minor damage	Minor cracking and spalling	Small soil or rock mass falls	<5	<3
ds_2 , moderate damage	Small cracking, spalling, and falling	Small soil or rock mass topple and sliding	5–10	3–30
ds_3 , extensive damage	Large cracking, spalling, and falling	Large slumps of soil or rock mass and deep sliding	>10	>30
ds_4 , collapse	Complete collapse	Complete collapse and landslide influence	-	-

earthquake intensities and soil-tunnel configurations, on the basis of a damage measure (DM) such as the exceedance of capacity bending moment or maximum axial stress [30]. Then, a probabilistic seismic demand model (PSDM) is constructed based on the calculated DM and the corresponding IM (e.g., Peak Ground Acceleration, PGA). Subsequently, fragility functions are generated based on the proposed PSDM [28,29]. A two-parameter lognormal probability distribution function is commonly adopted to describe the fragility for different damage states, as shown below:

$$P[ds \geq ds_i | IM] = \Phi \left[\frac{\ln(IM) - \ln(IM_{mi})}{\beta_{tot}} \right] \quad (1)$$

where Φ is the standard normal cumulative distribution function. IM_{mi} is the corresponding median value of IM at which the tunnel reaches the i th damage state, and β_{tot} is the total standard deviation. Specifically, for

tunnel structures, five limit states are usually defined corresponding to, i.e., no damage (ds_0), minor damage (ds_1), moderate damage (ds_2), extensive damage (ds_3), and collapse (ds_4) of the tunnel [27]. Table 1 summarizes potential patterns of damage on tunnels for various damage states, based on reported cases of damage during past earthquakes [27, 31,32].

2.3. Estimation of restoration times - restoration models

The time required to repair a tunnel and restore its functionality depends highly on the extent of damage, as well as on the availability of relevant resources, the management, and decision-making approaches in the inspection, design, and construction phases. To estimate recovery times, restoration models may be employed, which describe the rapidity of recovering the functionality (e.g. traffic) or the structural capacity of an infrastructure, that sustained a certain degree of damage due to an external cause (e.g., natural hazard) [33]. More specifically, the restoration models correlate the elapsed time after the initiation of restoration works, with the structural capacity gain and/or the functionality reached for a given damage level. They depend on the restoration or adaptation strategies for different hazard events. The existing restoration models are mainly developed based on expert judgment, and can be expressed by different shapes, such as linear, trigonometric [34], step-wise [35], or continuous [36] forms. Generally, the restoration process depends on the type of asset, the damage level, the availability of resources, and the prioritization of the owner’s goals.

Upon selection of an adequate restoration model and after defining the probability of occurrence of each damage state based on the fragility functions (step ii), the functionality function $Q(t)$ of a tunnel can be estimated following the approach proposed by FEMA [37], as a mean recovery weighted on each damage state probability. In this study, $Q(t)$ is defined as the average functionality of a tunnel during the recovery phase, as it is shown in Eq. (2). This approach is widely adopted in other similar resilience-related assessment research [38–40]. Based on this definition, the functionality function $Q(t)$ or resilience curve of the

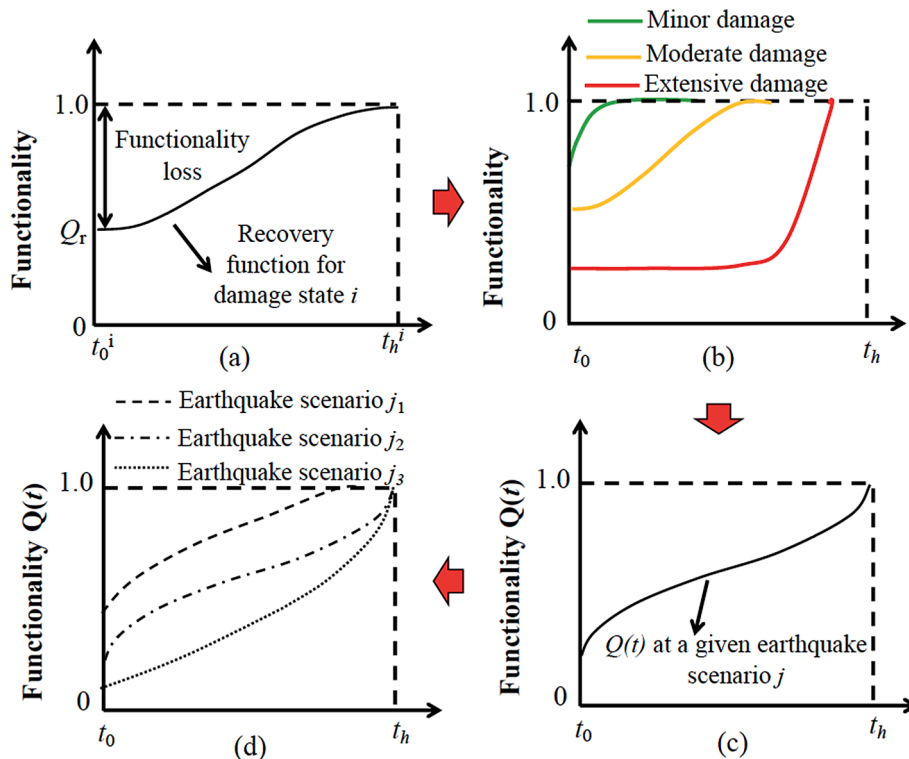


Fig. 2. Estimation of the functionality function $Q(t)$ of a tunnel: (a) functionality loss for the damage state i ; (b) restoration functions for different damage states; (c) average functionality of a tunnel at a given earthquake scenario j (see Section 2); (d) functionality function $Q(t)$ of a tunnel for different earthquake scenarios.

tunnel can be derived for a given level of seismic intensity, as presented in Fig. 2 and described in Section 3.3.1. The tunnel functionality function can take values between 0 and 1, and presents the characteristics of boundedness, monotonicity, and continuity [41]. A mathematical definition of the recovery process is provided by Cassottana et al. [41].

$$Q(t) = \sum_{i=0}^4 Q[ds_i|t]P[ds_i|IM] \tag{2}$$

where $Q(t)$ herein $Q[ds_i|t]$ represents the functionality of the tunnel being in DS_i , at time t after the start of restoration works, as defined by the restoration models. $P[ds_i|IM]$ represents the probability of occurrence of ds_i , computed using the fragility functions for a given IM level, as defined in the following equations:

$$P[ds_j|IM] = P[ds > ds_{j+1}|IM] - P[ds > ds_j|IM], \text{ when } j = 0, 1, 2 \tag{3}$$

$$P[ds_j|IM] = P[ds > ds_j|IM], \text{ when } j = 3 \tag{4}$$




where $P[ds > ds_j|IM]$ can be obtained from Eq. (1). It is noted that the existing fragility curves developed for the examined tunnel refer to minor damage, moderate damage and extensive damage. Therefore, the probability of occurrence of collapse $P[ds_4|IM]$ is not considered in the following analysis. Moreover, $P[ds_0|IM]$ is the probability of no damage state after the earthquake event, hence in Eq. (2) is multiplied by unity (1), that represents a full functionality.

To date, it is noted that a precise definition of functionality for tunnels of different use (e.g., utility, automotive, railway, metro) is not available. Following the illustration of FEMA [37], the interpretation of tunnel functionality can be described as follows: (i) 0–25% functionality – tunnel is likely to be non-functional, i.e., tunnel will be closed; (ii) 25–75% functionality – tunnel is likely to allow limited operations, i.e., part of the tunnel will be closed; (iii) 75–100% functionality – tunnel is likely to be functional, i.e., tunnel will be open. As an example, a tunnel with functionality equal to 66.7% generally indicates that the damaged tunnel is likely to allow limited operations. Yet, the decision to keep a tunnel open, partially open or closed, depends on its use, the operator’s policy, and safety thresholds, or the availability of alternative routes. In this paper, the post-event functionality at each DS was assumed to be 90% for DS_1 , 25% for DS_2 , 5% for DS_3 , and 0% for DS_4 , as per FEMA [37]. Further, for a long tunnel or a network of tunnels, the damage pattern and recovery are quite complex, considering that multiple damage locations of different intensities are possible. Recovery models should consider the distribution and severity of the damage, as well as the idle time before the commencement of any restoration works and the sequence of restoration tasks, which are related to engineering, operational, and organizational aspects.

A generic restoration model for tunnels provided by FEMA [37] is employed in this study (Fig. 1(ii)). Using Eq. (2), the functionality of a tunnel may be obtained over time for different damage states. Subsequently, the resilience analysis of the tunnel may be conducted (step iv). Due to the nature of the seismic hazard and its impact on the tunnel structure, the restoration process may have significant variations depending on the adopted strategy and available resources of the owners or stakeholders. For instance, the restoration time of the repair works can be to probabilistically modelled using a normal distribution. Therefore, future work should focus on the quantification of uncertainties associated with the recovery process, including probabilistic restoration functions needed [38,40,41].

It is noted that the restoration model describes the repair of structural damage, as defined by the fragility functions. The damage may include, for example, cracking of the lining, spalling of the concrete, cracking of the flooring, and dislocation. Damage to other installations and utilities such as signaling, communication or power supply, and railway tracks is not considered here. This type of damage can increase the required restoration time. Also, the idle time, i.e., the time before

Table 2
Definition of resilience grade.

Grade	Range	Colour
High resilience	$0.9 \leq R < 1.0$	
Moderate resilience	$0.6 \leq R < 0.9$	
Low resilience	$R < 0.6$	

any restoration work is commenced, is not taken into account. This time might include delays due to continuous seismic activity and aftershocks, inspection and safety assessments, site investigations, design of measures, and other organizational barriers.

2.4. Resilience analysis

This step combines the outcome of the vulnerability assessment of the examined tunnel (step i) with the restoration time for repairs and the recovery of functionality (step ii). In particular, the resilience curve defined by Eq. (2) and shown in Fig. 1 (iii) is employed to quantify resilience. The resilience index R given in Eq. (5) [14], is used herein, corresponding to the area under the resilience curve from time t_0 to t_h over this recovery time, i.e.:

$$R = \frac{\int_{t_0}^{t_h} Q(t)dt}{t_h - t_0} \tag{5}$$

where t_h is the time when the recovery is completed or another time frame for which the resilience analysis is conducted [11], t_0 is the time when the earthquake strikes, and $Q(t)$ is the functionality function, (see Eq. (2)).

It is noted that the resilience in this context describes the tunnel’s ability to withstand, respond and rapidly recover from a seismic event, and it is calculated on the basis of tunnel performance (robustness) and recovery time (rapidity). Moreover, the resilience index R given in Eq. (5) is defined as a summary resilience metric [42], and can be used to assess the current condition of an asset as well as the benefits of different design, restoration or adaptation strategies under various hazard events. Hence, the calculated resilience index R can support decision making by prioritizing a portfolio of assets (i.e., tunnel segments of an underground system or a highway network) based on the range of R values, similarly to risk metrics [43]. In this respect, the assets can be categorized into classes of low, moderate, or high resilience by setting appropriate thresholds of the R value for each class. These thresholds can be defined based on the distribution of the calculated R values (e.g., natural breaks classification), as well as based on the resilience objectives introduced by the infrastructure operators. The final decision should consider the direct (due to restoration works) and indirect losses (due to traffic interruptions or interdependencies) [44]. In this paper, three classes of resilience are defined, as shown in Table 2, to rank the tunnel under study for the different scenarios. In this way, the impact of different seismic intensities and tunnel conditions can be reflected in the resilience classification, which can provide meaningful and practical information in decision making, in particular for portfolios of assets. For instance, Low resilience indicates a more significant impact of the seismic loading, due to the tunnel’s higher vulnerability (lower robustness) and/or slower damage restoration (e.g., limited resources or other barriers in the recovery). Hence, the focus should be given to the assets with lower resilience, for a more detailed assessment and allocation of resources toward risk reduction.

3. Application

The framework described in Section 2 is applied herein to estimate the seismic resilience of typical circular tunnels in alluvial deposits for a

Table 3

Parameters of the fragility curves used in this study (median values are shown in columns 5, 6, 7 and standard deviation in column 8).

Reference	Tunnel typology	Soil type	Tunnel service time T (years)	Minor (g)	Moderate (g)	Extensive (g)	β_{tot}	
(1)	(2)	(3)	(4)	(5)	(6)	(7)	(8)	
Argyroudis and Pitilakis [27]	Shallow tunnel, diameter $d = 10$ m, burial depth $h = 10$ m	B	–	1.240	1.510	1.740	0.550	
		C	–	0.550	0.820	1.050	0.700	
		D	–	0.470	0.660	0.830	0.750	
Argyroudis et al. [45]	Shallow tunnel, diameter $d = 6$ m, burial depth $h = 10$ m, good construction quality	C	0	0.770	1.040	1.280	0.680	
			50	0.730	1.010	1.250	0.710	
			75	0.680	0.960	1.190	0.770	
		D	100	0.640	0.910	1.140	0.83	
			0	0.510	0.890	1.220	0.610	
			50	0.470	0.850	1.190	0.630	
		D	75	0.410	0.790	1.130	0.660	
			100	0.350	0.740	1.080	0.690	
			C	0	0.690	0.950	1.170	0.780
		D	Shallow tunnel, diameter $d = 6$ m, burial depth $h = 10$ m, poor construction quality	50	0.650	0.910	1.130	0.820
				75	0.610	0.870	1.100	0.880
				100	0.580	0.830	1.050	0.940
				0	0.250	0.610	0.910	0.760
				50	0.200	0.560	0.870	0.800
				75	0.150	0.510	0.820	0.850
D	Deep tunnel, diameter $d = 6.2$ m, burial depth $h = 30$ m	100	0.100	0.450	0.760	0.920		
		–	0.350	0.604	0.968	0.533		
		–	0.427	0.836	1.491	0.580		
Huang et al. [28]	Shallow tunnel, diameter $d = 6.2$ m, burial depth $h = 9$ m	D	–	0.350	0.604	0.968	0.533	
Moderately deep tunnel, diameter $d = 6.2$ m, burial depth $h = 20$ m	–	–	0.427	0.836	1.491	0.580		
Deep tunnel, diameter $d = 6.2$ m, burial depth $h = 30$ m	–	–	0.635	1.231	2.177	0.613		

range of seismic hazard scenarios. The effects of some critical parameters on tunnels' resilience, including soil conditions, tunnel burial depths, and construction quality of tunnels are examined and discussed in this application.

3.1. Selection of fragility functions

The development of fragility curves is the basis for the seismic risk and resilience of critical infrastructure. In recent decades, many studies focused on this research topic, including the development of several empirical and numerical fragility curves being considering different conditions and relevant parameters affecting the response, and hence, the vulnerability of tunnels under seismic shaking [e.g., 25–28, 32, 45–47]. Thorough reviews of the recent advances in the fragility analysis of tunnels and other underground structures may be found elsewhere [e.g., [48,49]]. The present application adopts a series of fragility curves for circular tunnels in alluvial deposits presented by the authors' previous work [27,28,45]. More specifically, Argyroudis and Pitilakis [27] provided fragility curves for shallow circular tunnels embedded in soil type B, C, and D of Eurocode 8 [50] based on the quasi-static approach. Extending the aforementioned study, Argyroudis et al. [45] developed a series of fragility curves for shallow circular tunnels constructed in soil type C and D, considering both the tunnel construction quality and the aging effects, using full dynamic analysis. Huang et al. [28] developed a series of fragility curves for typical shallow, moderately deep, and deep tunnels constructed in soil type D based on the full dynamic analysis method. The parameters (medians and total standard deviations β_{tot}) required to define these fragility models are shown in Table 3, and the corresponding fragility curves are shown in Fig. 3 for PGA (at the surface) values up to 1.6 g.

3.2. Selection of restoration models

The definition of restoration models is important for the quantification of resilience. Although the research on the modeling of infrastructure restoration is growing [51], to the authors' best knowledge, restoration data and models for circular tunnels subjected to ground seismic shaking are very limited in the existing literature. In this study, the restoration model for bored tunnels in the highway transportation

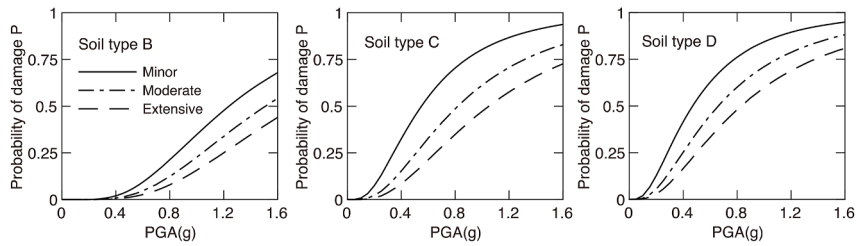
system proposed by the FEMA methodology [37], is used as an illustration. Table 4 shows the parameters, i.e., mean and standard deviation, of continuous restoration functions (all normal distribution functions) for a typical tunnel. The corresponding restoration curves for minor, moderate, and extensive seismic damage, shown in Fig. 4, follow FEMA [37]. It can be observed that the post-event functionality at each DS is about 90% for minor damage, 25% for moderate damage, and 5% for extensive damage. The tunnel functionality increases gradually as recovery time increases. According to this model, the full recovery (functionality of 100%) is achieved in about 3, 7, and 140 days for minor, moderate and extensive damage, respectively. It is noted that these restoration curves were developed based on the best fit to ATC-13 data [52], which was a result of an expert elicitation approach. Hence, a uniform distribution function is used to specify continuous recovery curves, while the recovery curves themselves are not probability density functions. The fragility curves for the herein examined tunnel refer to minor damage, moderate damage, and extensive damage. Therefore, the restoration curve for complete damage is not provided herein, and is not considered in the development of resilience curves and the calculation of the resilience index for the examined tunnel. A more rigorous restoration model for tunnels should be developed in the future, as discussed in Section 4.

3.3. Resilience assessment

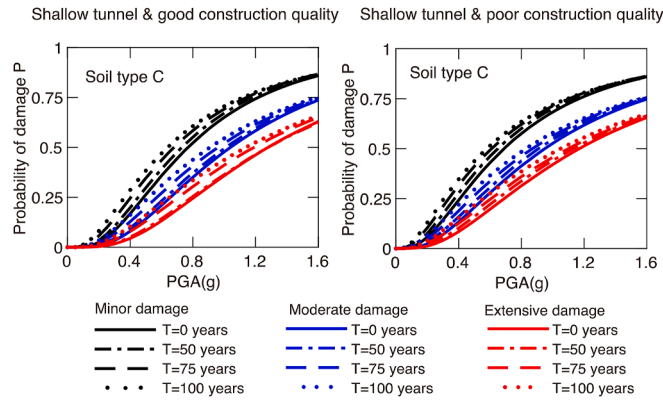
Using the general framework presented in Fig. 1 and the fragility and restoration models presented in Sections 3.1 and 3.2, resilience curves and indexes are generated for selected soil-tunnel configurations, while the effect of critical parameters is also investigated. It is noted that the time t_h in Eq. (5) is the time frame for which the resilience assessment is performed, in order to compare R values for different assets and/or different hazard scenarios, and is commonly determined as the maximum restoration time of the examined assets. In this paper, for the computation of the resilience index, time t_h corresponds to the recovery time for extensive damage [11], i.e., 140 days (Table 2).

3.3.1. Effect of soil conditions on seismic resilience of tunnels

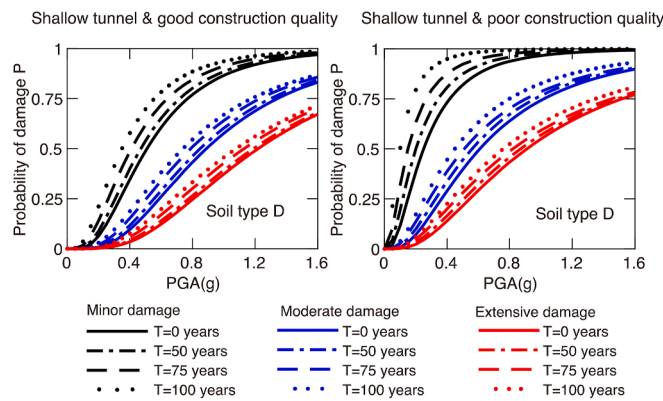
The effect of soil conditions is examined using the tunnel cases presented by Argyroudis and Pitilakis [27]. In particular, the analytical



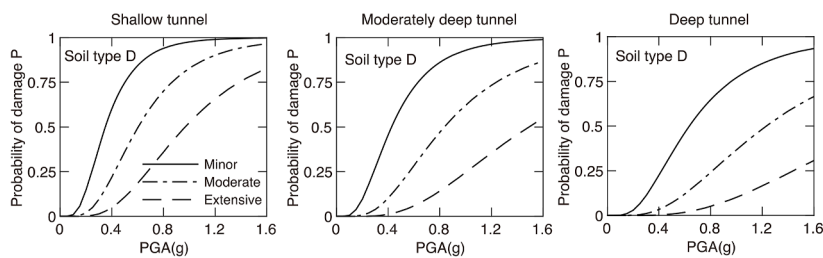
(a) Fragility curves of shallow circular tunnels provided by Argyroudis and Pitalakis [27].



(b) Time dependent fragility curves for shallow circular tunnels in soil type C Argyroudis et al. [45].



(c) Time dependent fragility curves for shallow circular tunnels in soil type D Argyroudis et al. [45].



(d) Fragility curves of circular tunnels in soil type D provided by Huang et al.

Fig. 3. Fragility curves provided by authors' previous work.

Table 4
Parameters of continuous restoration functions for circular tunnels [37].

Damage states	Mean (days)	Standard deviation σ (days)
Slight damage	0.5	0.3
Moderate damage	2.4	2.0
Extensive damage	45	30

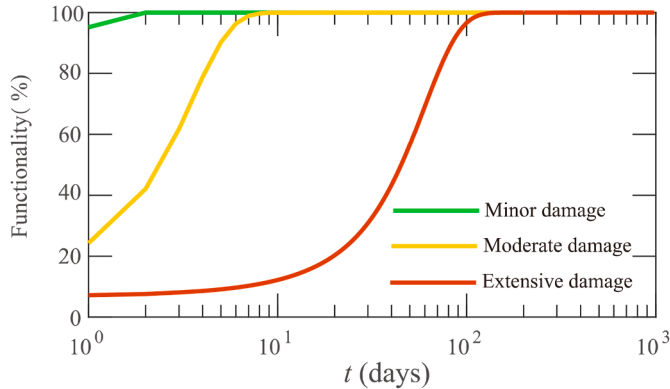


Fig. 4. Adopted tunnel restoration curves by FEMA [37].

fragility curves for shallow circular tunnels embedded in soil type B, C, and D, provided by Argyroudis and Ptilakis [27] (Fig. 3a), were used in the resilience analysis to evaluate the probability of occurrence of each damage state for five hazard scenarios (see step ii, Section 2) ranging from low to extreme seismic intensities (i.e., PGA equal to 0.2, 0.4, 0.6, 0.8 and 1.0 g). The functionality of the examined tunnel was then computed for each damage state and the selected seismic intensity using the restoration model presented in Table 4. Fig. 5 shows the resilience curves of the examined tunnel for the five shaking level intensities and for the cases where the tunnel was embedded in soil type B, C, and D. The post-event immediate residual functionality $Q(t = 0 \text{ day})$ of the tunnel decreases significantly as the seismic intensity level increases (i.e., as PGA moves from 0.2 g to 1.0 g) for all the examined soil conditions. Moreover, for the same seismic intensity level, the post-event immediate residual functionality $Q(t = 0 \text{ day})$ of the tunnel decreases as the soil becomes softer (i.e., from soil type B to D). Taking $PGA = 1.0 \text{ g}$ as an example, the residual functionality $Q(t = 0 \text{ day})$ of the tunnel is equal to 0.79, 0.45, and 0.35 for soil type B, C, and D, respectively. The above values indicate that the differences on the computed functionality of the same tunnel in different soil conditions can be more than 200%.

Moreover, it is observed that the slope of the resilience curve in Fig. 5 changes significantly around 3–5 days of the recovery process, while the tunnel recovers in about 90 days after the earthquake event regardless of the earthquake intensity. These results are associated with the definition of the resilience curve (see Eq. (5)), where the functionality of the tunnel

vs. time is calculated probabilistically for a given earthquake intensity, by considering the ‘contribution’ or ‘weight’ of the different damage states based on the corresponding damage probabilities as defined in the fragility curves. Therefore, the resilience curves show a weighted functionality considering all possible damage states for a given hazard intensity, while the restoration curves in Fig. 4 show the evolution of the functionality separately for each damage state. Based on the definition of the continuous restoration functions (Table 4), the recovery time for minor damage, moderate damage, and extensive damage is 3, 7, and 140 days, respectively. Hence, after 7 days, the functionality of the tunnel is expected to be 100% at both minor and moderate damage. Therefore, the resilience curve after this time is determined only by the restoration function of extensive damage. In this regard, the slope of the resilience curve in Fig. 5 changes significantly in about 3–5 days of the recovery process. Furthermore, it can be assumed that when the functionality of the tunnel is 95%, a full recovery has been almost achieved. After that point, the slope of the resilience curve is very small, and the curve tends to be asymptotic to the horizontal as per the definition of the restoration functions in Fig. 4. For example, in Fig. 5 for tunnels in soil type D, the recovery to 95% is reached in 2 days, 76 days, and 88 days for the scenarios of 0.2 g, 0.6 g, and 1.0 g. Also, for tunnels in soil type D, it is noted that, for intensities larger than 0.63 g, the recovery is dominated by the restoration of the extensive damage state, as the probability for this damage state is higher. More specifically, for a PGA equal to 0.63 g, the probabilities for no damage, minor damage, moderate damage, and extensive damage are equal to 0.348, 0.177, 0.119, and 0.357, respectively, based on Eqs. (3) and (4) and the corresponding fragility curves

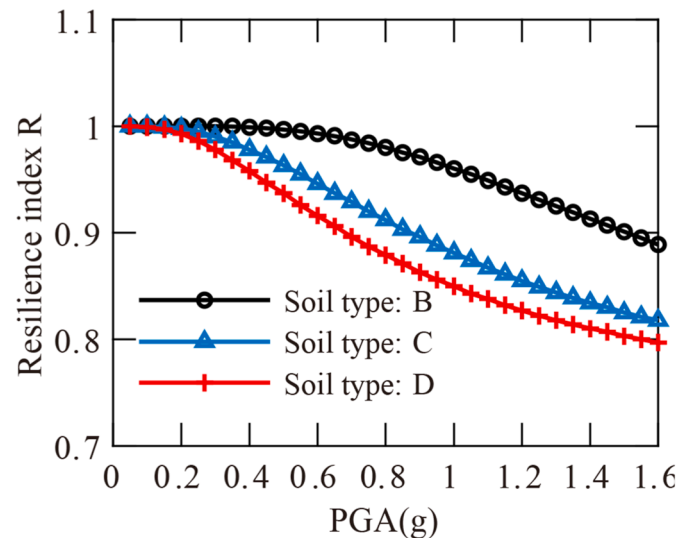


Fig. 6. Effect of soil conditions on the resilience index R of the examined tunnel.

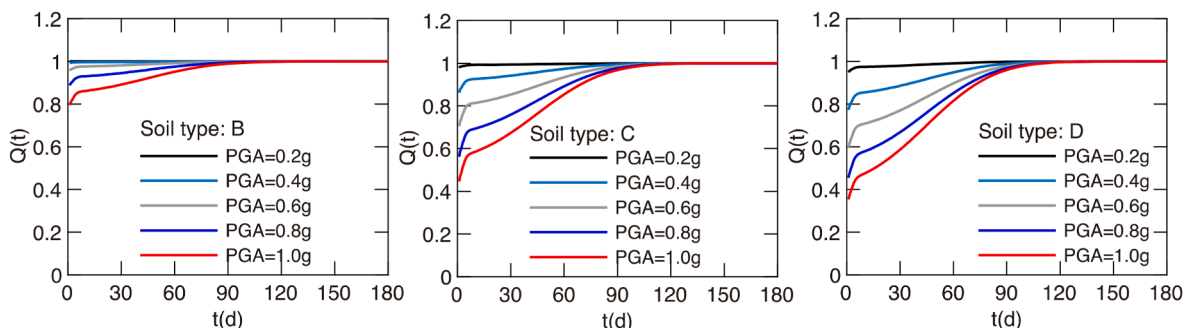


Fig. 5. Resilience curves showing the evolution of the recovery of functionality with time (in days) for shallow circular tunnels embedded in different soil types.

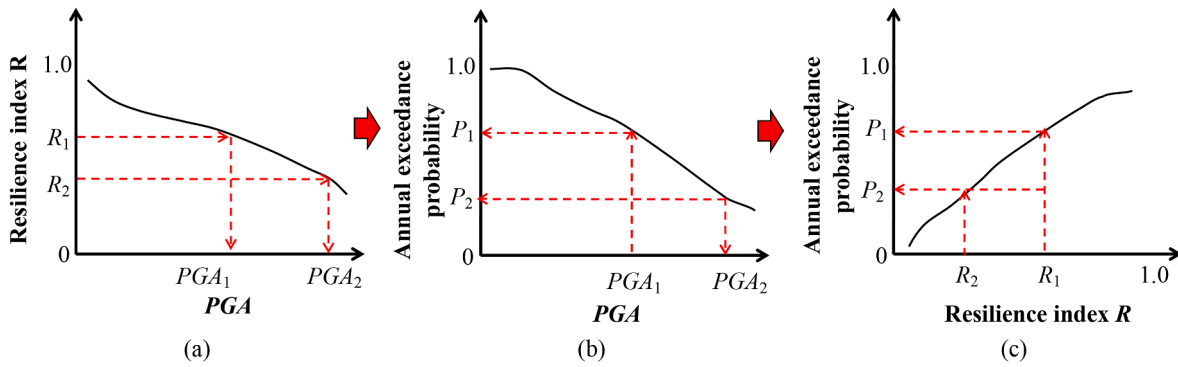


Fig. 7. Development of resilience index loss curve of the examined tunnels: (a) Resilience index curve; (b) Seismic hazard curve; and (c) Resilience curve in terms of annual exceedance probability of the resilience index.

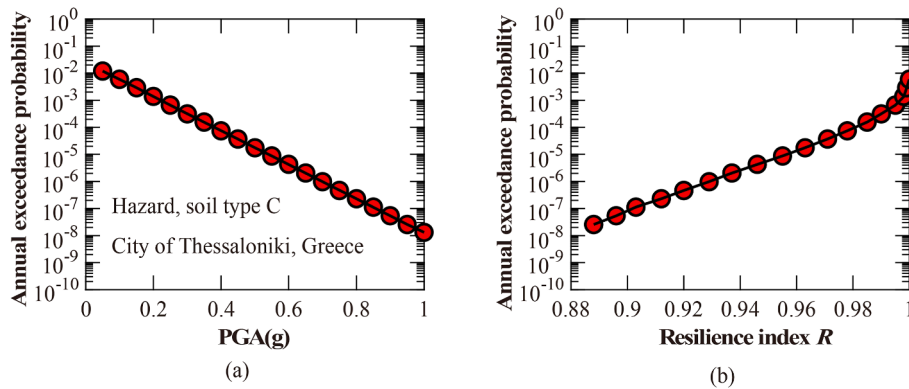


Fig. 8. Example of resilience index loss curve of tunnels in soil type C for the city of Thessaloniki, Greece: (a) Seismic hazard curve; and (b) Resilience curve in terms of annual exceedance probability of the resilience index.

by Argyroudis and Ptilakis [27].

The resilience index R of the examined tunnel is computed for the different soil conditions based on Eq. (5). Fig. 6 presents the evolution of the resilience index R with an increasing level of seismic intensity (i.e., expressed by means of PGA). The resilience index R is found to decrease significantly as the seismic intensity increases (i.e., R decreases as PGA increases from 0.1 g to 1.0 g). Moreover, lower values of R are estimated when the tunnel is embedded in softer soil deposits (i.e., lower values of R are computed from soil type B compared to soil type D), which indicates that tunnels embedded in stiff soil conditions are more robust and can generally absorb and withstand the effects of ground seismic shaking.

The resilience curve in terms of annual exceedance probability of the resilience index (R) can be plotted by integrating the resilience index (R) vs. the seismic intensity (PGA) curve and the corresponding seismic hazard curve (annual exceedance probability of PGA), as shown in

Fig. 7. As an example, the derived resilience index curve of tunnels in soil type C (Fig. 6), and the corresponding hazard curve for soil type C in the city of Thessaloniki, Greece (Fig. 8a) [53] are used to derive the exceedance probability curve for R shown in Fig. 8(b). Generally, it is found that the annual exceedance probability increases as the resilience index increases. This information can be used in conjunction with a given lifespan of the tunnel to facilitate decision making for asset management.

3.3.2. Effect of the burial depth on seismic resilience of tunnels

The burial depth of the tunnel plays a critical role in the seismic response of the soil-tunnel system, and therefore it has an important effect on the seismic resilience of tunnels. To examine this effect, the fragility curves developed by Huang et al. [28] for shallow, moderately deep, and deep circular tunnels embedded in soil type D are used herein (Fig. 3d).

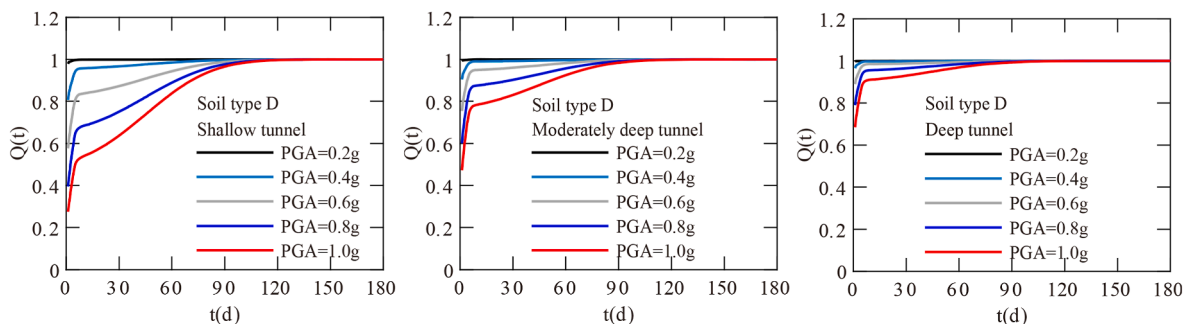


Fig. 9. Resilience curves showing the evolution of the recovery of functionality with time (in days) for circular tunnels with different burial depths in soil type D.

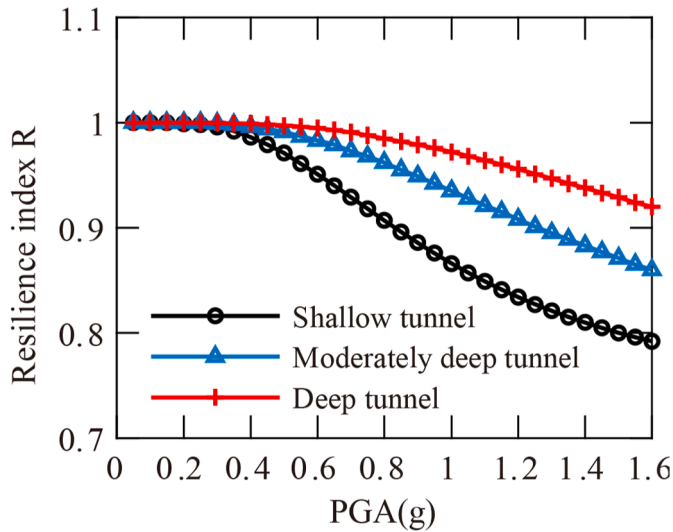


Fig. 10. Effect of tunnel burial depth on the computed resilience index R of the examined tunnels.

Fig. 9 shows the resilience curves of the examined circular tunnels with different burial depths in soil type D for the five shaking level intensities. The post-event immediate residual functionality $Q(t = 0 \text{ day})$ of the tunnel decreases significantly as the seismic intensity level increases for all the examined tunnels. Moreover, for the same seismic intensity level, the post-event immediate residual functionality $Q(t = 0 \text{ day})$ increases as the tunnel burial depth becomes deeper (i.e., from the shallow tunnel to the deep tunnel). Taking $PGA = 1.0 \text{ g}$ as an example, the residual functionality $Q(t = 0 \text{ day})$ of the tunnel is equal to 0.28, 0.47, and 0.69 for shallow tunnel, moderately deep tunnel, and deep tunnel, respectively. The above values indicate that the differences on the computed functionality of the tunnels in different burial depths can be up to 146%.

Fig. 10 presents the evolution of the resilience index R with increasing levels of seismic intensity (i.e., PGA), as computed for the examined soil-tunnel configurations, i.e., for a tunnel embedded in soil type D with various burial depths. The resilience index R is found to decrease as the seismic intensity increases, while lower R values are computed for the shallow tunnel case, compared to the cases where the tunnel is embedded in higher depths. This decrease in resilience is more evident in higher seismic intensities ($PGA > 0.8 \text{ g}$), while for PGA levels up to 0.4 g , the effect of burial depth on the resilience is minor. As an example, for a PGA equal to 0.35 g , the resilience index R is equal to 0.992, 0.995, and 0.998 for shallow, moderately deep, and deep tunnels, respectively. However, for a PGA equal to 1.0 g , the resilience index R is decreased to 0.886, 0.935, and 0.972 for minor, moderate and extensive damage, respectively. Therefore, for a given soil deposit and a given seismic intensity, the increase of the burial depth of a tunnel leads to a higher resilience of this tunnel against seismic ground shaking, in particular for high seismic intensities.

3.3.3. Effect of the tunnel construction quality on seismic resilience of tunnels

Evidently, the quality of construction of a tunnel is affecting its response against seismic hazards, and therefore, it affects its seismic resilience. To highlight this effect, the soil-tunnel configurations examined by Argyroudis et al. [45] were used herein. The study refers to shallow circular tunnels with good or poor construction quality embedded in soil type C or type D and different periods after the construction, to consider the impact of aging phenomena of the lining on the tunnels' fragility (Fig. 3b and c). In this section, the fragility curves for the initial design ($T = 0 \text{ years}$) are used in the resilience analysis (i.e., aging effects are ignored here).

Fig. 11 shows the resilience curves of the examined tunnels with different construction quality in soil types C and D for the five shaking level intensities. It is found that the post-event immediate residual functionality $Q(t = 0 \text{ day})$ of the tunnel decreases significantly as the seismic intensity level increases for all the examined tunnels in soil type C and D. As expected, for the same seismic intensity level, the post-event

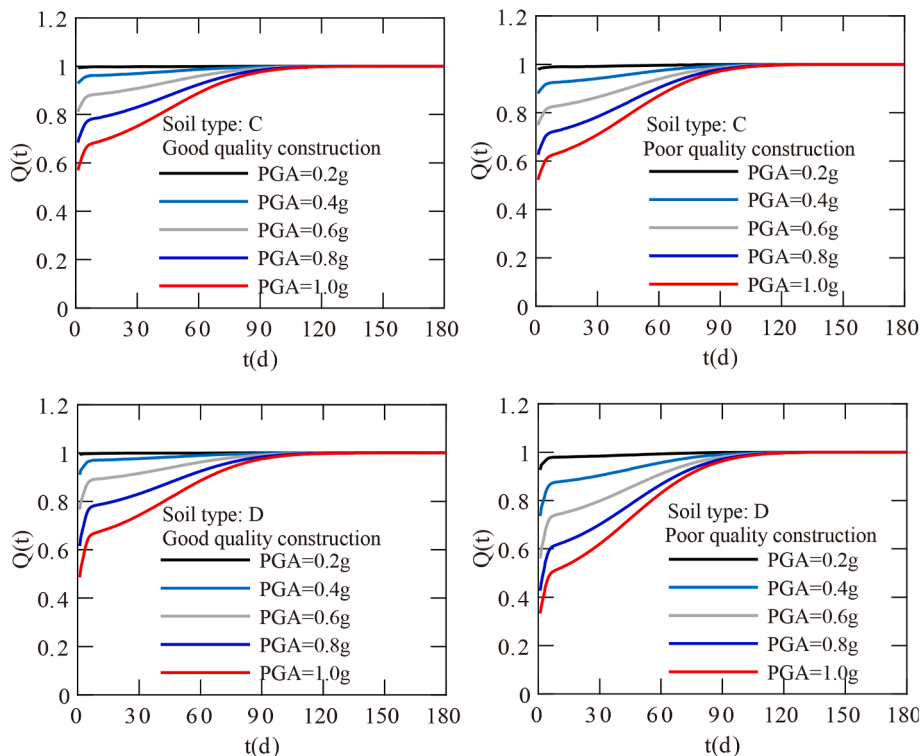


Fig. 11. Resilience curves showing the evolution of the recovery of functionality with time (in days) for circular tunnels with different construction quality.

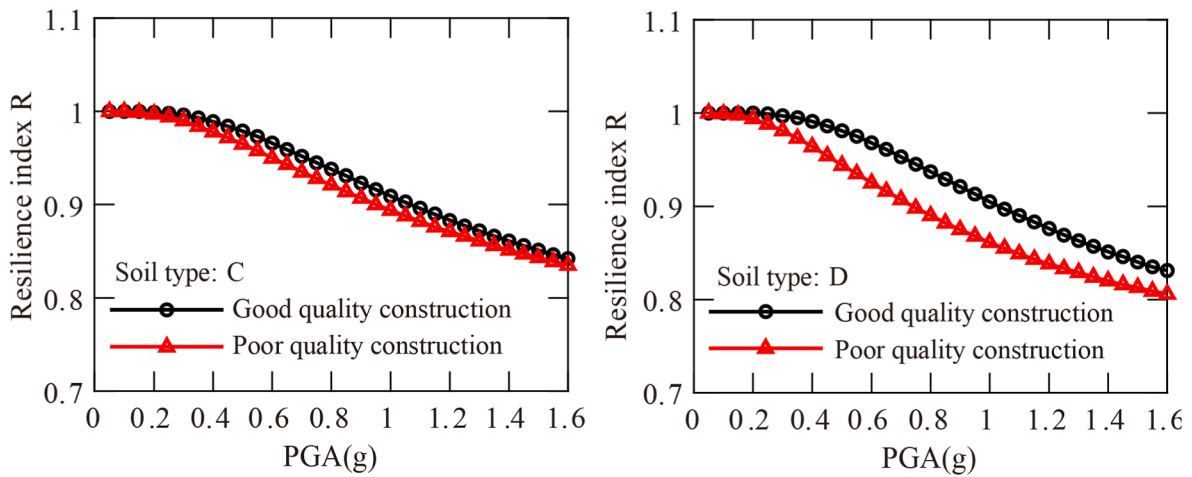


Fig. 12. Effect of construction quality of tunnels on the computed resilience index R.

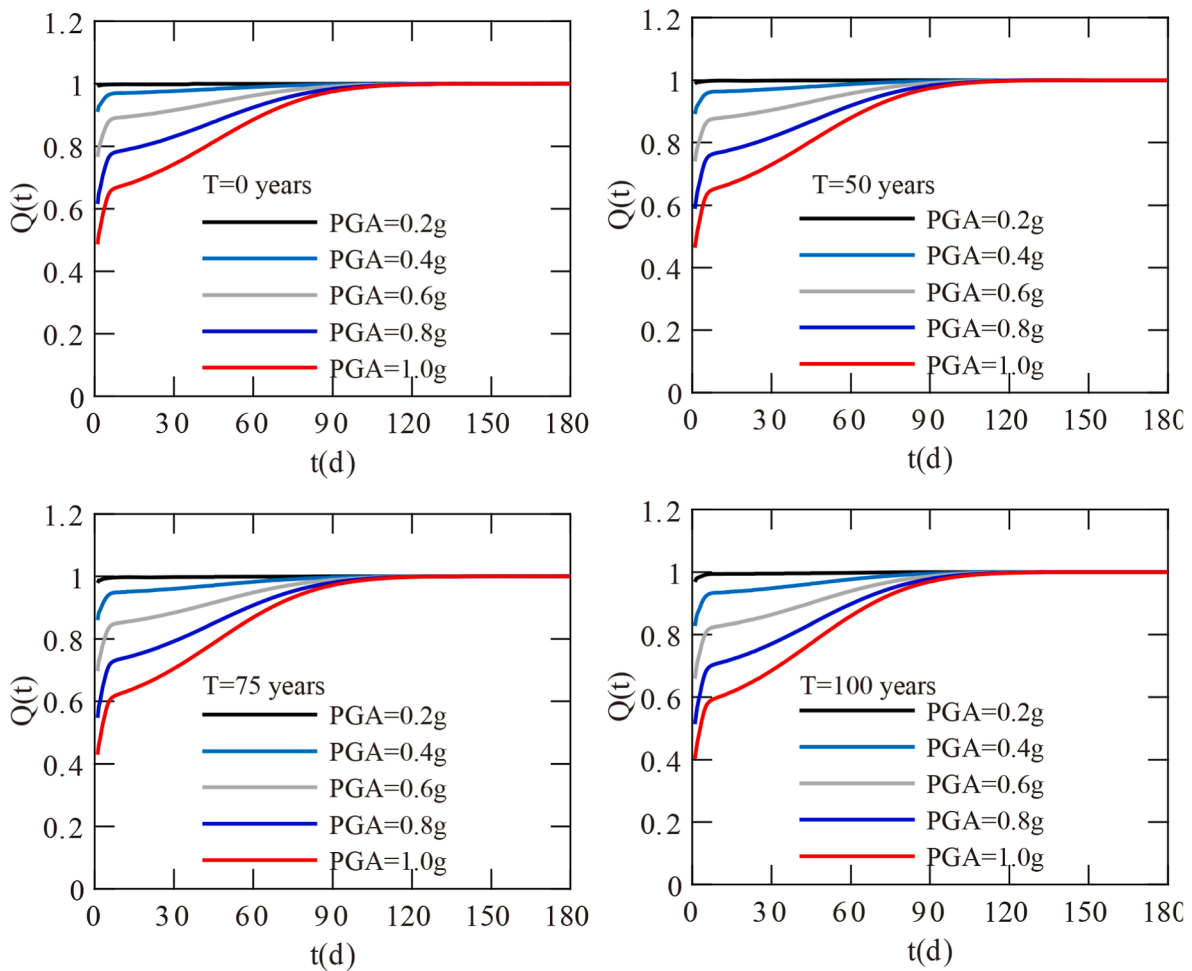
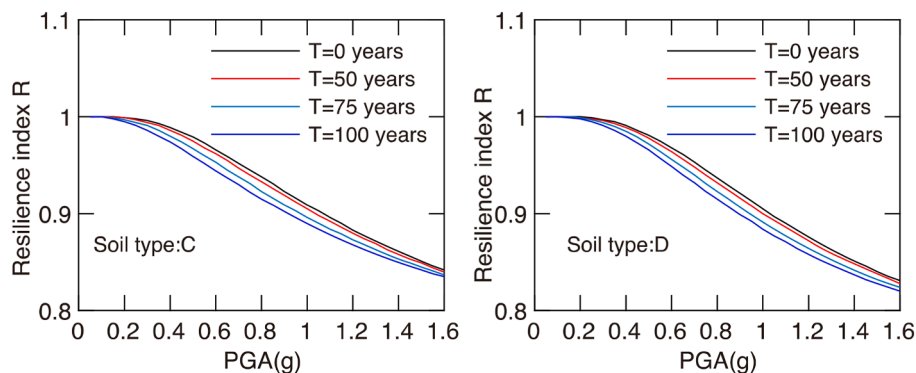


Fig. 13. Resilience curves showing the evolution of the recovery of functionality with time (in days) for circular tunnels in soil type D with good construction quality considering different service years.

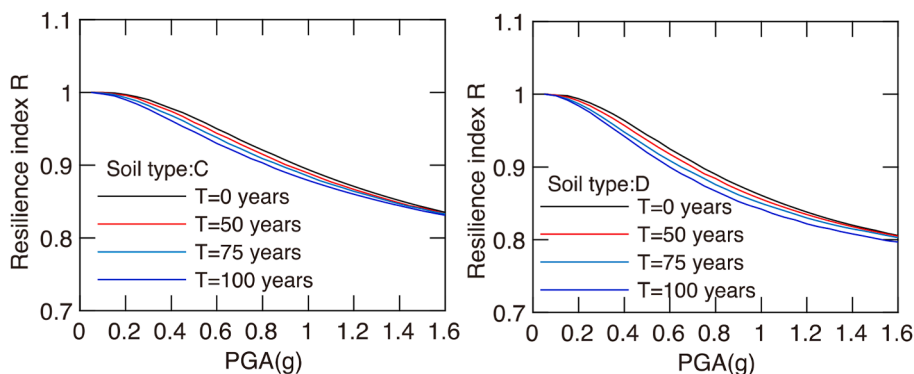
immediate residual functionality $Q(t = 0 \text{ day})$ of the tunnel with good quality construction is higher than the tunnel with poor quality construction. Taking $PGA = 1.0 \text{ g}$ and tunnel in soil type D as an example, the residual functionality $Q(t = 0 \text{ day})$ is equal to 0.49 and 0.33 for the tunnel with good quality construction and the tunnel with poor quality construction, respectively. These values indicate that the differences on the computed functionality of the tunnels with different construction

quality can be up to 48%.

Fig. 12 depicts the variation of the resilience index R with increasing level of seismic intensity (i.e., PGA), estimated for shallow circular tunnels with good or poor construction quality, embedded in soil type C or soil type D. In line with the observations made in the previous sections, the resilience index of the examined tunnels is found to decrease significantly as PGA increases from 0.1 g to 1.0 g. For a given seismic



(a) Shallow tunnel with good construction quality.



(b) Shallow tunnel with poor construction quality.

Fig. 14. Resilience index R of the circular tunnels considering different service years.

intensity, the resilience index of the tunnel with good construction quality is higher than the one estimated for the tunnel with poor construction quality. Moreover, it is clearly shown that the effect of the construction quality is more pronounced for PGA greater than 0.2 g when soil conditions are getting “softer” i.e., soil type D compared to soil type C. As an example, for a PGA equal to 1.2 g and in the case of soil type C, the resilience index R is equal to 0.883 and 0.871 for tunnels with good or poor-quality construction, respectively. However, for a PGA equal to 1.2 g and in the case of soil type D, the resilience index R is decreased to 0.876, and 0.838 for tunnels with good or poor-quality construction, respectively. The above results highlight the important role of tunnel construction quality in particular in the case of soft soil conditions.

3.3.4. Effect of aging phenomena of the lining on seismic resilience of tunnels

Tunnels are usually designed to properly and safely operate for a long-life span (e.g., over 100 years), however, their seismic performance may degrade gradually with time due to various progressive aging phenomena (e.g., corrosion). For better life-cycle management of deteriorating tunnel structures under lifetime hazards, it is extremely important to investigate the potential effect of aging phenomena on the seismic resilience of tunnels. To this end, the soil-tunnel configurations examined by Argyroudis et al. [45] were used herein. In particular, the time-dependent fragility curves (i.e., service years $T = 0, 50, 75,$ and 100 years) for shallow circular tunnels with good construction quality embedded in soil type C and soil type D (Fig. 3b and c) were used in the following resilience analysis.

Fig. 13 shows the resilience curves of the examined circular tunnels

in soil type D with good construction quality considering different service years for the five shaking level intensities. It is found that the post-event immediate residual functionality Q ($t = 0$ day) of the tunnel decreases significantly as the seismic intensity level increases for all the examined tunnels. Furthermore, for the same seismic intensity level, the post-event immediate residual functionality Q ($t = 0$ day) of the tunnel decreases as the service years increase (i.e., from 0 years to 100 years). For instance, for the scenario of $PGA = 1.0$ g, the residual functionality Q ($t = 0$ day) of the damaged tunnel is equal to 0.49, 0.46, 0.43, and 0.40 for 0 years, 50 years, 75 years, and 100 years, respectively. The above values indicate that the differences on the computed functionality of the tunnels with different service years can be more than 22.5%.

Fig. 14(a) and (b) show the evolution of resilience index R with increasing level of seismic intensity, as computed for the examined tunnels, considering also the quality of construction (i.e., good quality corresponds to higher strength properties of the lining). For a given level of seismic intensity, the resilience index R of the examined tunnel decreases with time; for instance, lower values are computed for R for the scenario of $T = 50$ years as compared to the one of $T = 0$ years. In other words, the seismic resilience of tunnels is found to decrease with increasing service time, due to the increasing effect of corrosion-related aging phenomena on the lining. The effect of increasing service time on seismic resilience of the examined tunnels is found to be more evident for the cases, where the tunnel is embedded in the softer soil deposit (i.e., soil type D).

4. Conclusions and recommendations for further investigation

This study presents a simple, feasible, and hence practical resilience

assessment framework for tunnels subjected to ground seismic shaking. The framework was applied for the case of circular tunnels in alluvial deposits. The effects of soil conditions, tunnel burial depths, the construction quality of tunnels, and aging phenomena, on tunnels' resilience, were evaluated and discussed based on the calculated resilience indexes. The results show that:

- (1) The seismic resilience of tunnels in alluvial (expressed in the form of a resilience index R) was found to decrease significantly with increasing levels of seismic intensity.
- (2) Tunnels embedded in stiffer soil deposits and at higher burial depths were found to be more resilient against the seismic hazard, i.e., these tunnels exhibit a higher ability to withstand and recover from earthquakes.
- (3) The resilience indexes of tunnels with good construction quality were generally higher than those estimated for tunnels with poor construction quality. This is more pronounced when the soil conditions are getting softer.
- (4) It is shown that the resilience decreases as tunnel service years increase due to the detrimental effects of materials' aging. Moreover, this aging effect is found to be more evident for the tunnel embedded in the softer soil deposit.

The benefits of different design parameters can be quantified through the resilience index, and such assessments can facilitate decision-making and prioritization, e.g., for risk mitigation, especially when dealing with large numbers of assets with different lifespans. It should be noted that all resilience analyses presented herein employed the restoration models proposed by FEMA [37]. However, there is a need for the development of rigorous restoration models, which will account for critical parameters, such as the type and extent of damage, the availability of resources, as well as the management approaches in construction and repairs in different countries, including lag times before the restoration works. The identification and quantification of uncertainties associated to the recovery process of tunnels is also a research priority and needs further investigation. In addition, the consideration of critical parameters affecting the seismic vulnerability of tunnels, for instance, erosion, corrosion, and other forms of chemical deterioration of the lining, may lead to a better estimation of the seismic vulnerability and hence, contribute toward better-informed resilience assessments.

Author statement

Zhongkai Huang: Conceptualization, Methodology, Formal analysis, Writing - Original draft, Writing - Review & Editing, Data curation, Visualization; Dongmei Zhang: Funding acquisition, Project administration, Supervision; Kyriazis Ptilakis: Review & Editing, Methodology, Supervision; Grigorios Tsinidis: Review & Editing; Hongwei Huang: Review & Editing; Dongming Zhang: Review & editing; Sotirios Argyroudis: Conceptualization, Methodology, Review & Editing, Supervision.

Declaration of competing interest

The authors declare that they have no known competing financial interests or personal relationships that could have appeared to influence the work reported in this paper.

Acknowledgments

The first and second authors acknowledge the financial support from the National Natural Science Foundation of China (Grants No. 52108381, 41772295, 51978517, 52090082), Shanghai Science and Technology Committee Program (Grants No. 21DZ1200601, 20DZ1201404), Innovation Program of Shanghai Municipal Education Commission (Grant No. 2019-01-07-00-07-456 E00051), National Key Research and Development Program of China (Grant No.

2021YFF0502200) and China Postdoctoral Science Foundation (Grant No. 2022T150484, 2021M702491).

References

- [1] Iida H, Hiroto T, Yoshida N, et al. Damage to Daikai subway station. *Soils Found* 1996;36(Special):283–300.
- [2] Shimizu M, Saito T, Suzuki A, Asakura T. Results of survey regarding damages of railroad tunnels caused by the Mid Niigata Prefecture Earthquake in 2004. *Tunn Undergr Space Technol* 2007;38(4):265–73.
- [3] Shen Y, Gao B, Yang X, Shuangjiang T. Seismic damage mechanism and dynamic deformation characteristic analysis of mountain tunnel after Wenchuan earthquake. *Eng Geol* 2014;180:85–98.
- [4] Wang TT, Kwok OLA, Jeng FS. Seismic response of tunnels revealed in two decades following the 1999 Chi-Chi earthquake (Mw 7.6) in Taiwan: a review. *Eng Geol* 2021;287:106090.
- [5] Callisto L, Ricci C. Interpretation and back-analysis of the damage observed in a deep tunnel after the 2016 Norcia earthquake in Italy. *Tunn Undergr Space Technol* 2019;89:238–48.
- [6] Roy N, Sarkar R. A review of seismic damage of mountain tunnels and probable failure mechanisms. *Geotech Geol Eng* 2017;35(1):1–28.
- [7] Cimellaro GP, Reinhorn AM, Bruneau M. Framework for analytical quantification of disaster resilience. *Eng Struct* 2020;32(11):3639–49.
- [8] Bruneau M, Chang SE, Eguchi RT, et al. A framework to quantitatively assess and enhance the seismic resilience of communities. *Earthq Spectra* 2003;19(4):733–52.
- [9] Sun W, Bocchini P, Davison BD. Resilience metrics and measurement methods for transportation infrastructure: the state of the art. *Sustainable Resilient Infrastruct* 2020;5(3):168–99.
- [10] Linkov I, Bridges T, Creutzig F, et al. Changing the resilience paradigm. *Nat Clim Change* 2014;4(6):407–9.
- [11] Argyroudis SA. Resilience metrics for transport networks: a review and practical examples for bridges. *Proc. Inst. Civ. Eng. Bridge Eng.* 2021. <https://doi.org/10.1680/jbren.21.00075>.
- [12] Markolf SA, Hoehne C, Fraser A, et al. Transportation resilience to climate change and extreme weather events—Beyond risk and robustness. *Transport Pol* 2019;74:174–86. <https://doi.org/10.1680/jbren.21.00075>.
- [13] Ayyub BM. Practical resilience metrics for planning, design, and decision making. *ASCE-ASME J. Risk Uncertainty Eng. Syst. Part A: Civ Eng* 2015;1(3):04015008.
- [14] Ayyub BM. Systems resilience for multihazard environments: definition, metrics, and valuation for decision making. *Risk Anal* 2014;34(2):340–55.
- [15] Yang DY, Frangopol DM. Life-cycle management of deteriorating civil infrastructure considering resilience to lifetime hazards: a general approach based on renewal-reward processes. *Reliab Eng Syst Saf* 2019;183:197–212.
- [16] Anwar GA, Dong Y, Zhai C. Performance-based probabilistic framework for seismic risk, resilience, and sustainability assessment of reinforced concrete structures. *Adv Struct Eng* 2020;23(7):1454–72.
- [17] Ekhlaspour A, Raissi DM, Eghbali M, Samadian D. Pre-event assessment of seismic resilience index for typical Iranian buildings via a web-based tool. *Int J Civ Eng* 2021;1–16.
- [18] Argyroudis SA, Mitoulis SA, Hofer L, Zanini MA, Tubaldi E, Frangopol DM. Resilience assessment framework for critical infrastructure in a multi-hazard environment: case study on transport assets. *Sci Total Environ* 2020;714:136854.
- [19] Chienkuo C, Eiki Y, Santoso D. Seismic resilience analysis of a retrofit-required bridge considering moment-based system reliability. *Struct. Infrastruct. Eng.* 2021;17(6):757–78.
- [20] Alipour A, Shafei B. Seismic resilience of transportation networks with deteriorating components. *J Struct Eng* 2016;142(8):C4015015.
- [21] Capacci L, Biondini F, Titi A. Lifetime seismic resilience of aging bridges and road networks. *Struct. Infrastruct. Eng.* 2002;16(2):266–86.
- [22] Panteli M, Mancarella P, Trakas DN, et al. Metrics and quantification of operational and infrastructure resilience in power systems. *IEEE Trans Power Syst* 2017;32(6):4732–42.
- [23] Huang H, Zhang D. Resilience analysis of shield tunnel lining under extreme surcharge: characterization and field application. *Tunn Undergr Space Technol* 2016;51:301–12.
- [24] Ansal A, Kurtuluş A, Tönük G. Seismic microzonation and earthquake damage scenarios for urban areas. *Soil Dynam Earthq Eng* 2010;30(11):1319–28.
- [25] Huang ZK, Ptilakis K, Argyroudis S, et al. Selection of optimal intensity measures for fragility assessment of circular tunnels in soft soil deposits. *Soil Dynam Earthq Eng* 2021;145:106724.
- [26] Anderson DG, Martin GR, Lam I, et al. Seismic analysis and design of retaining walls, buried structures, slopes, and embankments, vol. 611. *Transportation Research Board*; 2008.
- [27] Argyroudis SA, Ptilakis KD. Seismic fragility curves of shallow tunnels in alluvial deposits. *Soil Dynam Earthq Eng* 2012;35:1–12.
- [28] Huang ZK, Ptilakis K, Tsinidis G, et al. Seismic vulnerability of circular tunnels in soft soil deposits: the case of Shanghai metropolitan system. *Tunn Undergr Space Technol* 2020;98:103341.
- [29] Huang Z, Argyroudis SA, Ptilakis K, et al. Fragility assessment of tunnels in soft soils using artificial neural networks. *Undergr Space* 2022;7(2):242–53. <https://doi.org/10.1016/j.undsp.2021.07.007>.
- [30] Tsinidis G, Karatzetzou A, Stefanidou S, et al. Developments in seismic vulnerability assessment of tunnels and underground structures. *Geotechnics* 2022;2(1):209–49.

- [31] Andreotti G, Lai CG. Use of fragility curves to assess the seismic vulnerability in the risk analysis of mountain tunnels. *Tunn Undergr Space Technol* 2019;91:103008.
- [32] ALA. Seismic fragility formulations for water systems: Part 1-guideline. American Society of Civil Engineers-FEMA; 2001.
- [33] Mitoulis SA, Argyroudis SA, Loli M, et al. Restoration models for quantifying flood resilience of bridges. *Eng Struct* 2021;238:112180.
- [34] Bocchini P, Frangopol DM. Optimal resilience-and cost-based postdisaster intervention prioritization for bridges along a highway segment. *J Bridge Eng* 2012;17(1):117–29.
- [35] Padgett J, DesRoches R. Bridge functionality relationships for improved seismic risk assessment of transportation networks. *Earthq Spectra* 2007;23(1):115–30.
- [36] Bocchini P, Deco A, Frangopol D. Probabilistic functionality recovery model for resilience analysis. In: Biondini F, Frangopol D, editors. *Bridge maintenance, safety, management, resilience and sustainability*. London: Taylor and Francis Group; 2012.
- [37] FEMA. Hazus 4.2 SP3: hazus earthquake model technical manual. FEMA; 2020.
- [38] Argyroudis SA, Mitoulis SA, Hofer L, et al. Resilience assessment framework for critical infrastructure in a multi-hazard environment: case study on transport assets. *Sci Total Environ* 2020;714:136854.
- [39] Pang Y, Wang X. Cloud-IDA-MSA conversion of fragility curves for efficient and high-fidelity resilience assessment. *J Struct Eng* 2021;147(5):04021049.
- [40] Decò A, Bocchini P, Frangopol DM. A probabilistic approach for the prediction of seismic resilience of bridges. *Earthq Eng Struct Dynam* 2013;42(10):1469–87.
- [41] Cassottana B, Shen L, Tang LC. Modeling the recovery process: a key dimension of resilience. *Reliab Eng Syst Saf* 2019;190:106528.
- [42] Poulin C, Kane MB. Infrastructure resilience curves: performance measures and summary metrics. *Reliab Eng Syst Saf* 2021;216:107926.
- [43] Poulin C, Kane MB. Infrastructure resilience curves: performance measures and summary metrics. *Reliab Eng Syst Saf* 2021;216:107926.
- [44] Xofi M, Domingues JC, Santos PP, et al. Exposure and physical vulnerability indicators to assess seismic risk in urban areas: a step towards a multi-hazard risk analysis. *Geomatics, Nat Hazards Risk* 2022;13(1):1154–77.
- [45] Argyroudis SA, Nasiopoulos G, Mantadakis N, Mitoulis SA. Cost-based resilience assessment of bridges subjected to earthquakes. *Int. J. Disaster Resilience Built Environ.* 2020;12(2). <https://doi.org/10.1108/IJDRBE-02-2020-0014>.
- [46] Argyroudis S, Tsinidis G, Gatti F, et al. Effects of SSI and lining corrosion on the seismic vulnerability of shallow circular tunnels. *Soil Dynam Earthq Eng* 2017;98:244–56.
- [47] Huang G, Qiu W, Zhang J. Modelling seismic fragility of a rock mountain tunnel based on support vector machine. *Soil Dynam Earthq Eng* 2017;102:160–71.
- [48] de Silva F, Fabozzi S, Nikitas N, et al. Seismic vulnerability of circular tunnels in sand. *Geotechnique* 2020:1–15.
- [49] Tsinidis G, de Silva F, Anastopoulos I, et al. Seismic behaviour of tunnels: from experiments to analysis. *Tunn Undergr Space Technol* 2020;99:103334.
- [50] CEN. EN 1998-1. Eurocode 8 design of structures for earthquake resistance. Brussels, Belgium: European Committee for Standardisation; 2004.
- [51] Martell M, Miles S, Choe Y. Modeling of lifeline infrastructure restoration using empirical quantitative data. 2020. [https://doi.org/10.1061/\(ASCE\)NH.1527-6996.0000514](https://doi.org/10.1061/(ASCE)NH.1527-6996.0000514).
- [52] ATC. Earthquake damage evaluation data for California. Applied Technology Council; 1985.
- [53] Pitolakis K, Cultrera G, Margaris B, et al. Thessaloniki seismic hazard assessment: probabilistic and deterministic approach for rock site conditions. In: 4th International conference on earthquake geotechnical engineering; 2007. paper no 1701.